PERFORMANCE OF SCAFFOLD FRAME SHORING UNDER PATTERN LOADS AND LOAD PATHS

By J. L. Peng,[1] T. Yen,[2] Y. Lin,[3] K. L. Wu,[4] and W. F. Chen[5]

ABSTRACT: This research examines the behavior of a large full-scale scaffold frame shoring subjected to pattern loads with various load paths. In this test program, sand bags were placed on the top of the scaffold frame shoring to simulate the weight of fresh concrete during construction. The routes of placing sand bags are based on the paths of placing fresh concrete in actual construction sites. The test results show that the axial tube forces of scaffolds just below the location of a newly placed sand bag increase sharply. In addition, the axial tube forces do not change significantly when sand bags are placed at other positions on formwork during the load path. It is shown that the effect of influence surfaces on the scaffold frame shoring is not apparent during the placing of sand bags. In addition, the maximum axial tube force of a scaffold subjected to different load paths is very close to the maximum axial tube force of this specific scaffold after the completion of the loading path. Thus, a typical uniform load as used for an applied concrete load in design can replace the actual fresh concrete pattern load during construction. Both lateral forces acted at the top of a scaffold frame shoring and the sidesway of scaffolds are small during tests. The regions of some larger axial forces in the scaffold frame shoring vary in different load paths.

INTRODUCTION

High-clearance reinforced-concrete buildings such as warehouses, museums, gymnasia, or churches generally have a large region for placing fresh concrete during construction. In this region, the effect of placed concrete patterns with various load paths on formwork and temporary structures has not been systematically studied. Most of the current design codes focus on ensuring the safety of buildings during their service lives such as considering the maximum wind load or earthquake force acting on the buildings, and so on. Relatively speaking, there is a shortage of research in the safety of temporary structures for high-clearance buildings during construction. Because of the lack of the research, the current available codes do not provide enough information for the safety of temporary structures.

During construction reinforced-concrete buildings typically use temporary structures to support construction loads on formwork. These temporary structures are removed when the concrete attains the required strength. Thus, the proper design of temporary structures may be ignored due to their temporary nature. Since scaffolds used as temporary structures are economical and easily installed, they are widely used in high-clearance buildings during construction.

Construction loads of buildings mainly include fresh concrete, formwork, steel, equipment, crews, and so on. The placed fresh concrete makes up a large proportion of construction loads (Yen et al. 1993). Furthermore, the fresh concrete on formwork also has the characteristics of load patterns. Previous research on load patterns (Jirsa et al. 1969; Jofriet and McNeice 1971) have focused on the mechanical behavior of slabs with a specific loading position during the service life of a structure, i.e., evaluating maximum bending moment at a specific point in the slab. There is little information on the influence of the placement concrete patterns on temporary supports and formwork during construction. Based on the investigations of construction accidents in the United States and in Taiwan (Hadipriono and Wang 1986; Yen et al. 1991), formwork collapses in high-clearance structures usually occurred during fresh concrete placement, and not after the completion of the placement procedure. In actual construction sites, placements of fresh concrete must consider the load paths during construction. This is quite different from the uniform load assumption typically used in design. Current codes and design guidelines do not consider the pattern loads and load paths of fresh concrete. Most of the collapses of temporary structures are associated with the effects of the concrete pattern load on temporary structures. In fact, many collapses of temporary structures occur during construction. These collapses often lead to failure of the entire structure and cause the death of work crews.

This research uses a full-scale test to investigate the mechanical behavior of a typical temporary structure, the scaffold frame shoring, subjected to sand bag pattern load with various load paths. The safety procedures developed based on the test results can be used to reduce the possible collapse accidents in construction.

RESEARCH OBJECTIVES

This research investigates the relationship between the scaffold frame shoring and different pattern load paths by measuring the change of axial tube forces of the scaffolds during the placing of concrete. The objectives can be summarized as follows:

1. To investigate the effect of influence surfaces (Peng et al. 1996c) on scaffold frame shoring by measuring the change of axial tube force of scaffolds.
2. To investigate the lateral forces induced by pattern loads at the top restrained formwork in the scaffold frame shoring. Thus, the effect of pattern loads on the scaffold frame shoring can be predicted.
3. To investigate the difference between the uniform load used in design, and the pattern load, which actually acted on the scaffold frame shoring during construction.
4. To investigate the regions of larger axial forces of the scaffold frame shoring with different load paths.
5. To investigate the lateral displacement of the scaffold frame shoring with different load paths.

[1]Assoc. Prof., Dept. of Constr. Engrg., Chaoyang Inst. of Technol., Taiwan, ROC.
[2]Prof., Dept. of Civ. Engrg., Nat. Chung-Hsing Univ., Taiwan, ROC.
[3]Assoc. Prof., Dept. of Civ. Engrg., Nat. Chung-Hsing Univ., Taiwan, ROC.
[4]Grad. Res., Dept. of Civ. Engrg., Nat. Chung-Hsing Univ., Taiwan, ROC.
[5]Head of Struct. Engrg., School of Civ. Engrg., Purdue Univ., West Lafayette, IN 47907.

Note. Discussion open until November 1, 1997. To extend the closing date one month, a written request must be filed with the ASCE Manager of Journals. The manuscript for this paper was submitted for review and possible publication on March 25, 1996. This paper is part of the ***Journal of Construction Engineering and Management***, Vol. 123, No. 2, June, 1997. ©ASCE, ISSN 0733-9364/97/0002-0138–0145/$4.00 + $.50 per page. Paper No. 12930.

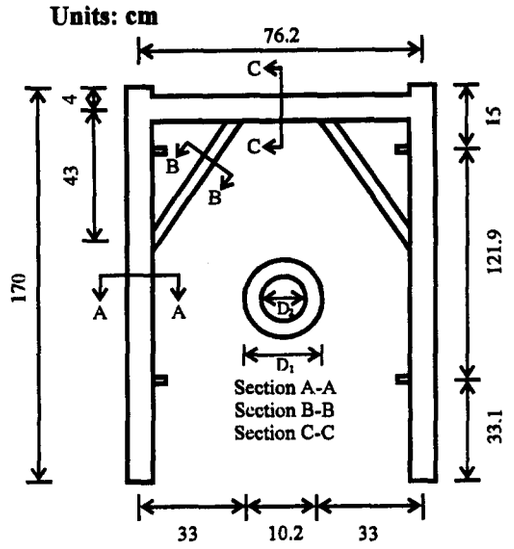

Cross Section	D_1(cm)	D_2(cm)	A(cm^2)	I(cm^4)	J(cm^4)
A-A	4.30	3.86	2.82	5.88	11.77
B-B	2.70	2.40	1.20	0.98	1.96
C-C	4.30	3.86	2.82	5.88	11.77
Cross Brace	2.15	1.8	0.92	0.44	0.88

FIG. 1. Dimensions of Portal Type Scaffold Frame

DIMENSIONS AND MATERIAL PROPERTIES OF SCAFFOLDS

The scaffold used in tests is the portal-type scaffold. Fig. 1 shows the dimensions of the scaffold frame. The material properties measured in the laboratory test are: (1) E (elastic modulus) = 1.92 × 10^6 kgf/cm^2 (18.83 × 10^6 N/cm^2); (2) ν (Poisson ratio) = 0.27; (3) F_y (yielding stress) = 5,150 kgf/cm^2 (50,506 N/cm^2); and (4) F_u (ultimate stress) = 6,450 kgf/cm^2 (63,255 N/cm^2).

TEST SETUP

Resistance Part

This test uses a three-bay, five-row, three-story full-scale scaffold frame shoring as shown in Fig. 2. The supporting floor of the test is a reinforced-concrete slab with a thickness of 40 cm and strength of 4,000 psi. Adjustable shoring heads are installed at the top of the third floor scaffolds. The stringers are placed on the top of adjustable shoring heads. Finally, formwork typically used in construction sites of Taiwan is placed on the stringers. This temporary structure assembly is based on the actual installation procedure used in Taiwan. In addition, the top boundary of the scaffold frame shoring is restrained by a frame instead of hardened reinforced-concrete walls and columns. The frame consists of eight vertical I-shaped steel columns and four horizontal I-shaped beams fixed at the reinforced-concrete base with anchor bolts. Some tubes with strain gauges placed at opposite sites are horizontally installed between the frame and formwork. Thus, the horizontal lateral forces of the scaffold frame shoring can be measured during different load paths as shown in Fig. 3. Fig. 4 shows the configuration of the three-bay, five-row, three-story scaffold frame shoring.

The failure of the scaffold frame shoring mainly occurred in the plane of the scaffold based on the indoor experimental results (Yen et al. 1993). Therefore, the measurement of lateral force of the system is focused on the in-plane behavior with the top being restrained. Thus, it can be used directly to check the indoor experimental tests.

The key points of measurement are axial forces and lateral displacements of the scaffolds. The strain gauges were glued to the opposite sides of each tube at the bottom of the second

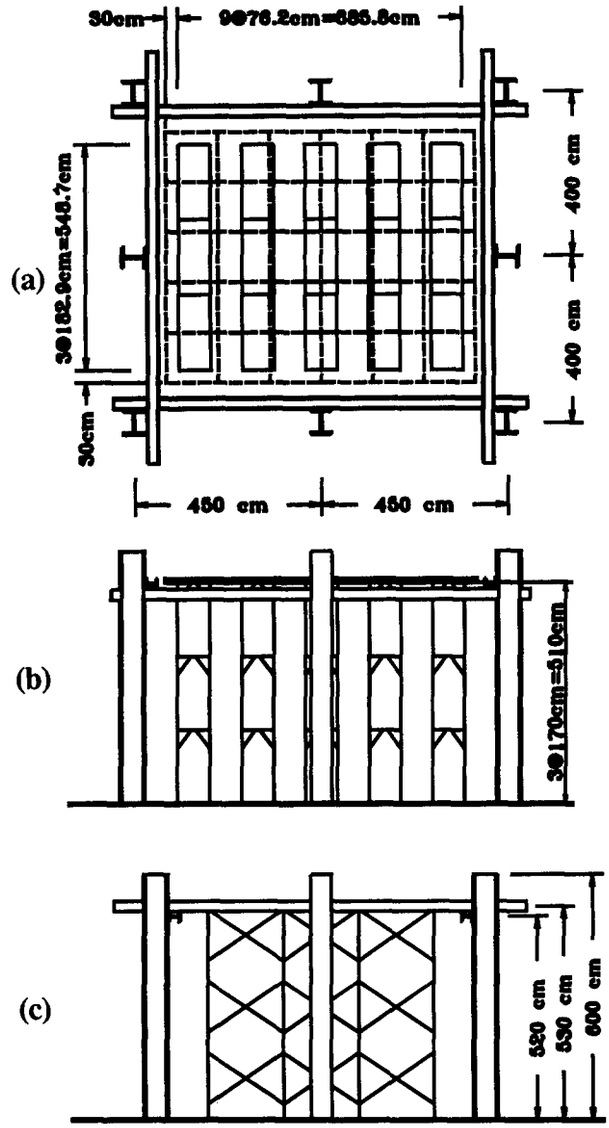

FIG. 2. Configurations and Dimensions of Full-Scale Scaffold Frame Shoring

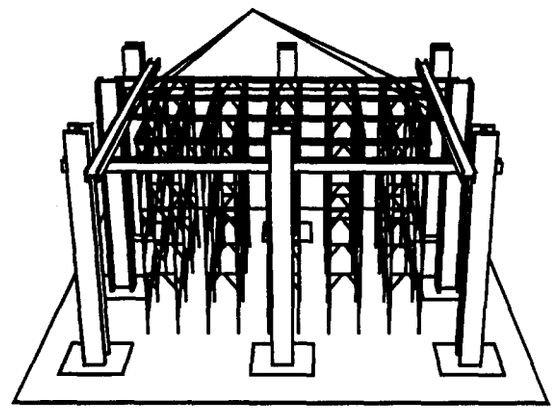

FIG. 3. Measuring Points for Lateral Forces in Full-Scale Scaffold Frame Shoring

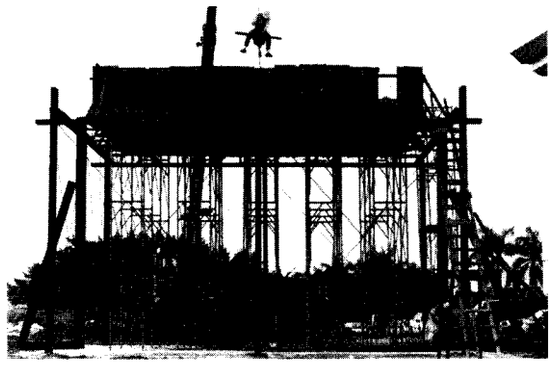

FIG. 4. Placing Sand Bags on Scaffold Frame Shoring in Load Path Tests

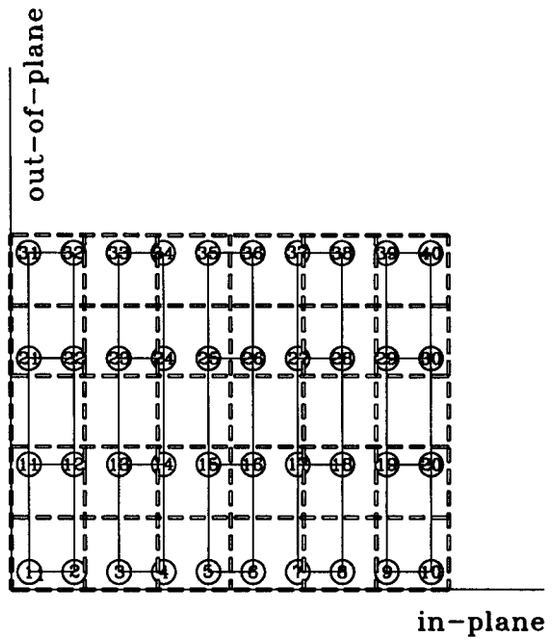

FIG. 5. Tube Positions, Tube Numbers, and Sand Bag Blocks in Load Path Tests

floor scaffolds for all 40 tubes. The measured positions of lateral displacement were chosen at some specific places in plane and out of the plane of the scaffold frame shoring based on previous tests and theoretical analyses (Yen et al. 1993; Peng 1994; Peng et al. 1996a; Pent et al. 1996b). The rules used to record sidesway by theodolites were fixed at the top of the first-floor scaffold. All data were recorded after the sand bags were placed on the formwork. Sand bags were placed one at a time on the formwork and the data were recorded five times continuously in every two seconds. For convenience, all tubes of scaffolds were marked from 1 to 40 as shown in Fig. 5. Two video cameras were placed in the positions in the plane and out of the plane of the system to record the entire process of this test.

Load Part

There were 30 blocks painted on the formwork before the tests as shown in Fig. 5. All sand bags were placed in the specified block. The weight of each sand bag was 750 kgf (7,355 N). After all sand bags were placed on the formwork, the total load on the formwork was equal to the weight of a concrete slab with a thickness of about 20 cm [0.206 m = (0.75 × 30)/(2.4 × 7.46 × 6.09)].

The routes of placing sand bags were based on investigations in actual construction sites (Yen et al. 1993). All 30 sand bags were sequentially placed at the specified positions following a given load path. All sand bags were removed from the formwork to the ground after a load path test was complete. The recording system was reset before the next test started.

TEST RESULTS AND ANALYSIS

Maximum Axial Force

Position of Maximum Axial Force

The load paths used in tests are illustrated in Fig. 6, load paths, A, B, and C, which are typically used in concrete placement in Taiwan. Fig. 7 shows a total of 30 sand bags being placed on formwork. There are six load stages in tests. Any stage needs to place five sand bags at specified positions of formwork in a load path.

Figs. 8–10 show the distribution and tendency of axial forces of scaffolds for load paths A, B, and C, respectively. As shown in Figs. 8–10, (a–f) show the distribution of axial forces at different stages. In these figures, the values on the ordinate are the axial tube forces evaluated based on the readings of strain gauges, and those on two perpendicular abscissas are the geometrical positions of scaffolds. During the test, the magnitudes of axial forces reflect the distribution and positions of placed sand bags. No significant changes in axial forces are found at positions without sand bags.

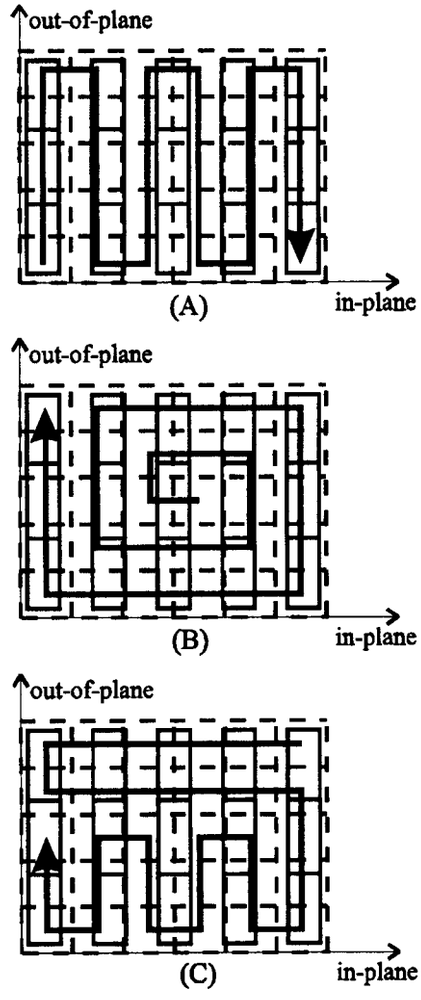

FIG. 6. Paths of Placed Sand Bags in Load Path Tests

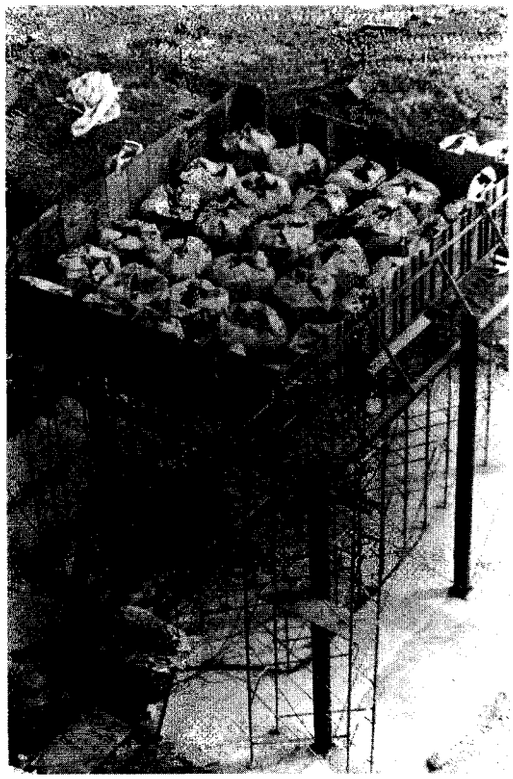

FIG. 7. Distributions of Sand Bags Placed on Scaffold Frame Shoring in Load Path Tests

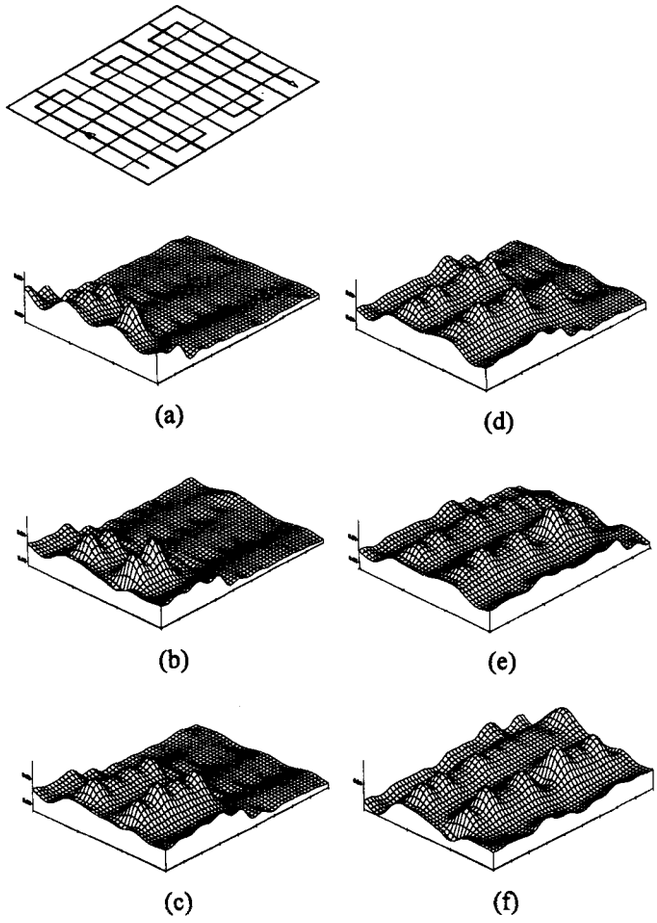

FIG. 8. Axial Tube Force Tendencies of Scaffolds in Load Path A

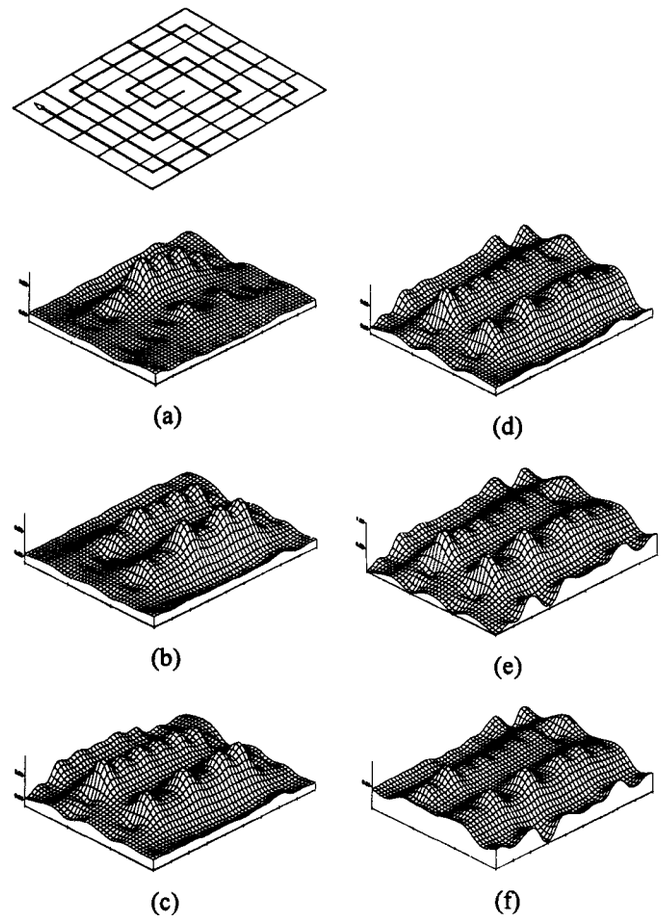

FIG. 9. Axial Tube Force Tendencies of Scaffolds in Load Path B

Tables 1–3 show the four largest axial forces in scaffold tubes for each loading stage as loads were placed in paths A, B, and C, respectively. The first column in Tables 1–3 shows the total numbers of sand bags placed on the formwork. The second column shows the tube numbers and values (in t) of the largest axial force produced by the number of sand bags shown in column 1. The third gives the same data for the second largest axial force at any given loading stage. The fourth and fifth columns are for the third and fourth largest ones, respectively, at any given loading stage. The relationship between axial forces and numbers of total sand bags is shown in Figs. 11–13. In these figures, the ordinate is axial tube forces, and the abscissa is the number of placed sand bags. On the basis of these tables and figures, the maximum axial tube force of scaffolds occurs during the loading process but not at the end of load placement. For example, the maximum axial tube force in load path A locates at tube number 23 when the eighth sand bag is placed on the formwork (Table 1). The maximum axial tube force in load path B locates at tube number 15 and the 25th sand bag (Table 2). The maximum axial tube force of load path C locates at tube number 15 and 24th sand bag (Table 3).

Relationship Between Maximum Axial Force and Pattern Loads

Current design codes do not focus on the pattern load of fresh concrete during construction. Thus, for convenience in design, uniform load is generally used. The ratio of the maximum axial force during a load path to that when the placement is complete shows the effect of pattern load on the scaffold frame shoring.

J. Constr. Eng. Manage., 1997, 123(2): 138-145

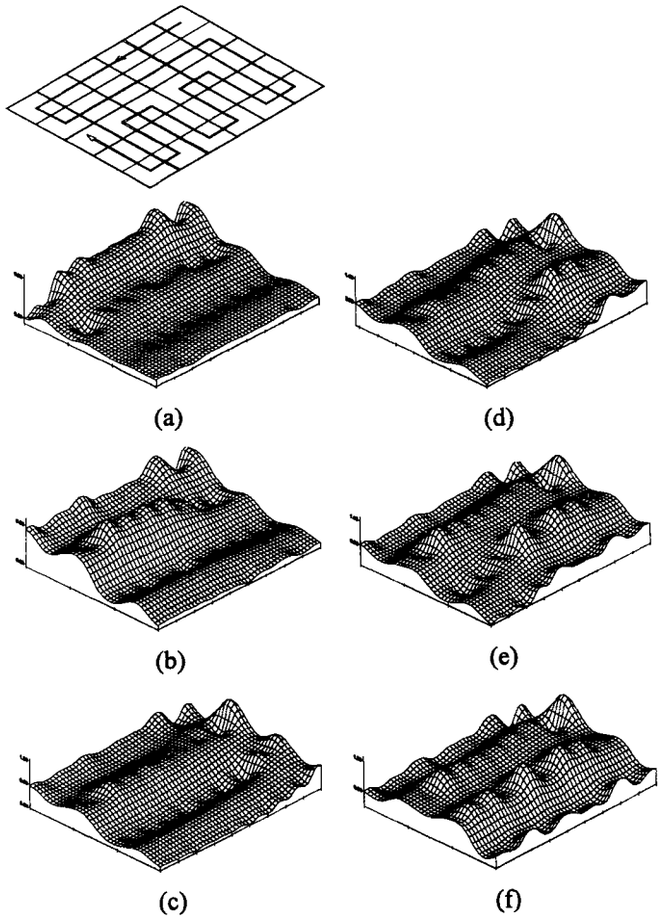

FIG. 10. Axial Tube Force Tendencies of Scaffolds in Load Path C

TABLE 1. Four Largest Axial Tube Forces in Load Path A

Total number of sand bags (1)	First		Second		Third		Fourth	
	Tube number (2)	Axial force (t) (3)	Tube number (4)	Axial force (t) (5)	Tube number (6)	Axial force (t) (7)	Tube number (8)	Axial force (t) (9)
0	1	0	2	0	3	0	4	0
1	1	0.306	2	0.208	23	0.154	11	0.13
2	1	0.422	12	0.403	23	0.387	2	0.336
3	12	0.65	11	0.463	23	0.376	1	0.368
4	12	0.658	11	0.476	22	0.452	21	0.411
5	12	0.62	22	0.487	21	0.482	23	0.455
6	12	0.628	23	0.598	22	0.558	21	0.479
7	23	1.048	22	0.715	12	0.639	21	0.485
8	23	*1.364*	22	0.782	12	0.696	21	0.474
9	23	*1.364*	22	0.766	12	0.736	13	0.723
10	23	1.318	13	0.891	12	0.791	22	0.753
11	23	1.327	13	0.907	12	0.75	22	0.747
12	23	1.318	13	0.896	12	0.739	22	0.731
13	23	1.302	13	0.883	22	0.728	12	0.726
14	23	1.302	13	0.877	15	0.755	14	0.728
15	23	1.308	13	0.874	15	0.731	14	0.728
16	23	1.32	13	0.873	22	0.716	14	0.715
17	23	1.327	13	0.872	22	0.715	14	0.709
18	23	1.332	13	0.874	25	0.747	22	0.715
19	23	1.305	13	0.861	15	0.793	25	0.747
20	23	1.318	13	0.866	15	0.818	26	0.747
21	23	1.294	13	0.85	15	0.828	25	0.717
22	23	1.291	13	0.847	15	0.82	25	0.72
23	23	1.31	17	0.864	13	0.855	15	0.826
24	23	1.31	17	0.994	13	0.853	15	0.815
25	23	1.31	17	0.991	13	0.866	15	0.818
26	23	1.302	17	0.994	13	0.858	15	0.815
27	23	1.294	17	0.958	13	0.847	15	0.793
28	23	1.294	17	0.961	13	0.869	15	0.807
29	23	1.321	17	0.977	13	0.888	15	0.831
30	23	1.348	17	0.977	13	0.893	15	0.839

TABLE 2. Four Largest Axial Tube Forces in Load Path B

Total number of sand bags (1)	First		Second		Third		Fourth	
	Tube number (2)	Axial force (t) (3)	Tube number (4)	Axial force (t) (5)	Tube number (6)	Axial force (t) (7)	Tube number (8)	Axial force (t) (9)
0	1	0.079	27	0.046	18	0.041	3	0.038
1	17	0.26	26	0.181	15	0.143	27	0.138
2	15	0.395	25	0.282	17	0.265	26	0.222
3	25	0.693	24	0.36	15	0.36	26	0.279
4	25	0.747	26	0.704	27	0.376	15	0.368
5	25	0.734	26	0.661	27	0.601	15	0.363
6	25	0.731	27	0.701	26	0.663	28	0.642
7	18	0.826	25	0.731	27	0.693	26	0.674
8	17	0.82	18	0.758	25	0.731	27	0.652
9	15	0.901	17	0.801	18	0.763	25	0.701
10	15	0.891	17	0.818	18	0.769	25	0.693
11	15	0.874	17	0.807	13	0.793	18	0.78
12	15	0.877	17	0.812	18	0.785	23	0.761
13	23	0.923	15	0.885	17	0.815	18	0.772
14	23	0.937	15	0.847	17	0.815	24	0.793
15	23	0.937	15	0.842	25	0.815	17	0.807
16	23	0.953	15	0.847	27	0.796	25	0.793
17	23	0.94	17	0.799	18	0.771	25	0.763
18	23	0.934	15	0.845	25	0.801	24	0.788
19	23	0.948	15	0.855	25	0.804	24	0.791
20	23	0.939	15	0.85	25	0.809	24	0.788
21	23	0.942	15	0.858	17	0.812	25	0.812
22	23	0.945	18	0.907	17	0.855	15	0.853
23	23	0.948	17	0.918	18	0.912	15	0.88
24	15	1.002	23	0.956	17	0.92	18	0.904
25	15	*1.012*	23	0.92	17	0.918	18	0.888
26	15	1.007	23	0.923	17	0.915	13	0.899
27	15	1.002	13	0.91	23	0.91	17	0.904
28	15	0.999	23	0.942	17	0.912	13	0.91
29	15	0.999	23	0.956	18	0.91	17	0.91
30	15	0.999	23	0.969	17	0.915	18	0.912

TABLE 3. Four Largest Axial Tube Forces in Load Path C

Total number of sand bags (1)	First		Second		Third		Fourth	
	Tube number (2)	Axial force (t) (3)	Tube number (4)	Axial force (t) (5)	Tube number (6)	Axial force (t) (7)	Tube number (8)	Axial force (t) (9)
0	7	0.011	10	0.008	12	0.008	4	0.005
1	40	0.417	30	0.116	39	0.108	38	0.095
2	38	0.55	40	0.42	39	0.16	30	0.16
3	38	0.55	40	0.417	37	0.374	36	0.265
4	38	0.547	40	0.411	37	0.357	36	0.352
5	38	0.541	34	0.409	40	0.395	33	0.357
6	38	0.558	40	0.409	34	0.393	31	0.379
7	38	0.547	31	0.452	21	0.411	40	0.411
8	23	0.585	38	0.547	34	0.447	31	0.436
9	23	0.606	24	0.55	38	0.55	34	0.498
10	23	0.604	25	0.552	24	0.547	38	0.547
11	38	0.623	23	0.606	24	0.552	25	0.547
12	30	0.701	38	0.636	23	0.615	25	0.555
13	30	0.991	38	0.642	23	0.62	24	0.555
14	30	0.991	38	0.655	20	0.625	23	0.623
15	30	0.977	20	0.709	38	0.658	23	0.623
16	30	0.969	20	0.701	38	0.65	23	0.617
17	30	0.983	20	0.709	38	0.65	23	0.633
18	30	0.966	18	0.918	28	0.78	19	0.712
19	30	0.969	18	0.883	27	0.826	28	0.774
20	30	0.988	17	0.942	18	0.885	27	0.799
21	17	1.007	30	0.985	18	0.88	27	0.788
22	17	1.002	30	1.002	18	0.901	27	0.788
23	30	0.999	28	0.996	15	0.991	16	0.899
24	15	*1.045*	30	1.004	17	0.985	18	0.912
25	15	1.034	30	1.002	17	0.985	23	0.907
26	15	1.029	17	1.002	30	0.996	23	0.918
27	15	1.01	30	0.996	17	0.994	18	0.912
28	15	1.023	30	1.002	17	0.999	18	0.91
29	15	1.018	30	1.007	17	1.004	13	0.907
30	15	1.029	17	1.012	30	1.01	18	0.918

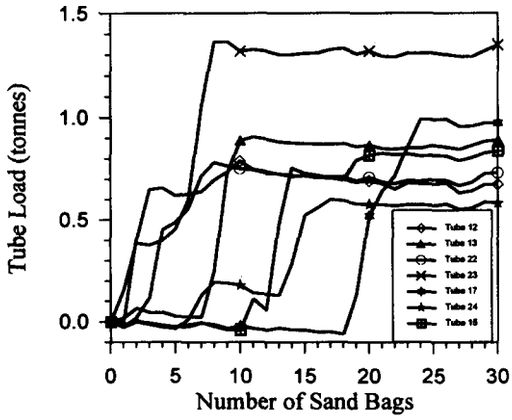

FIG. 11. Larger Axial Tube Forces of Scaffolds in Load Path A

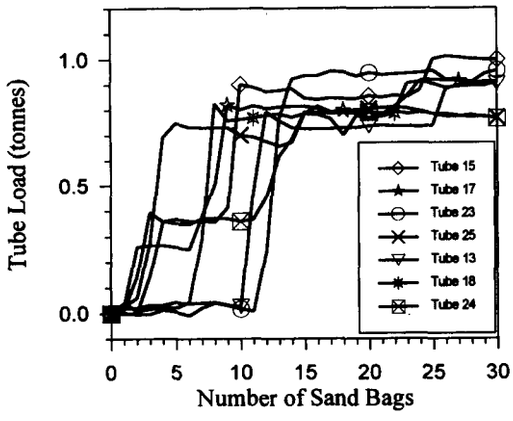

FIG. 12. Larger Axial Tube Forces of Scaffolds in Load Path B

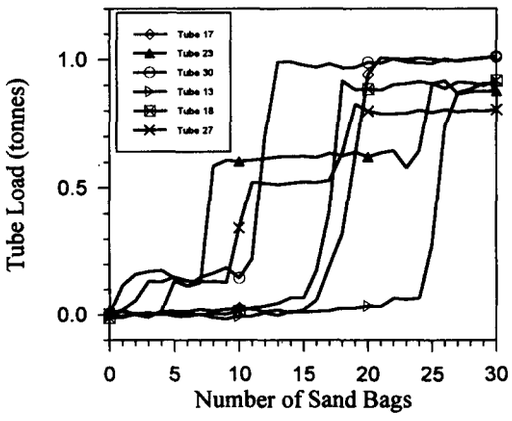

FIG. 13. Larger Axial Tube Forces of Scaffolds in Load Path C

As shown in Table 1 for load path A, the maximum axial tube force is 1.364 t at tube number 23 when the eighth sand bag is placed on formwork during load path. On the other hand, the axial force is 1.348 t at tube number 23 when total sand bags (30 sand bags) are completely placed on formwork. Thus, the nonuniform factor (NF) can be found as

load path A: NF = 1.364/1.348 = 1.01

As shown in Tables 2 and 3, the NF for load paths B and C are

load path B: NF = 1.012/0.999 = 1.01

load path C: NF = 1.045/1.029 = 1.02

They are very close to 1. In this case, the pattern load is not important, and the uniform load can be used to replace the pattern load for construction design.

Check of Influence Surfaces

Figs. 11–13 show a sudden increase of axial tube forces with load paths A, B, and C when the sand bag is being placed at a specified position on the formwork. This sudden change of axial tube force is due to the positions of sand bags. Generally speaking, the axial tube force of scaffolds beneath the placed sand bag has a tendency to increase suddenly as soon as this sand bag is placed on the formwork. Furthermore, once this axial tube force is increased, it will not be reduced with sand bags placed in other places.

When load patterns are placed on formwork during load paths, the scaffold frame shoring should theoretically have the effect of influence surfaces since the scaffold frame shoring is an indeterminate structure (Peng et al. 1996a,b,c). However, on the basis of test results, the axial forces in shoring legs do not apparently change during tests.

The concept of influence surfaces is found insignificant in load paths for the following two reasons: (1) the formwork and stringers in the scaffold frame shoring are not really continuous, so the influence surfaces do not have a global effect on the system; and (2) the effect of influence surfaces is lim-

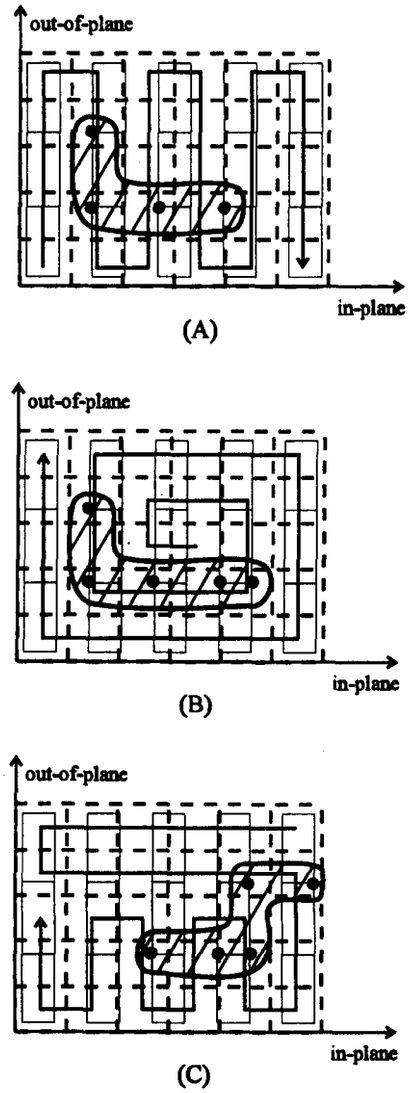

FIG. 14. Regions of Large Axial Tube Forces in Load Paths A, B, and C

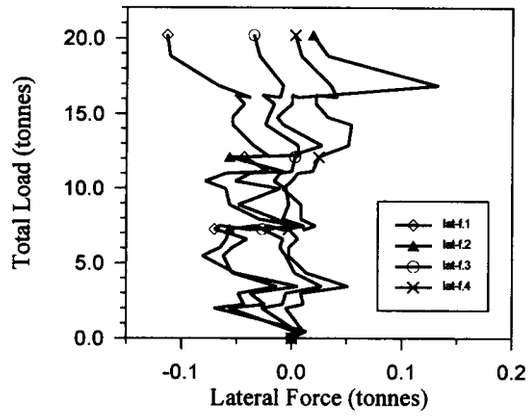

FIG. 15. Lateral Forces Recorded in Scaffold Frame Shoring in Load Path A

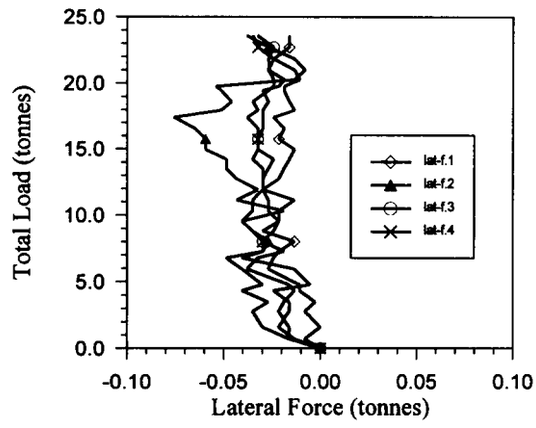

FIG. 16. Lateral Forces Recorded in Scaffold Frame Shoring in Load Path B

ited in a small area since the function of influence surfaces of the system may converge very fast.

Region of Larger Axial Forces

Tables 1–3 show no significant difference between the largest value of axial force and other larger values (2nd, 3rd, etc.) of axial forces in the scaffold frame shoring. If positions of these large values are close, all these values can be considered equal. This is because the variances of all these values may be larger than the difference among them. Thus, the region covering these positions can be considered a dangerous area. The regions of large axial forces are shown in Fig. 14 for load paths A, B, and C separately. The region of tube numbers 13, 15, 17, and 23 has larger axial forces in the load path A, the region of tube numbers 13, 15, 17, 18, and 23 has large axial forces in the load path B, and the region of tube numbers 15, 17, 18, 28, and 30 has large axial forces in the load path C. These regions can be used as observational places for checking a possible dangerous condition of the system during placement of fresh concrete.

Lateral Forces and Displacements of Scaffolds

The lateral forces measured are shown in Figs. 15–17 for load paths A, B, and C, respectively. In these figures, the abscissa is lateral forces, and ordinate is total load measured from strain gauges. The measured lateral forces are small compared with the total loads with different load paths. Furthermore, the lateral displacements are almost nothing in the in-plane and out-of-plane directions of the scaffold frame shoring based on the observation of theodolites. This is because the

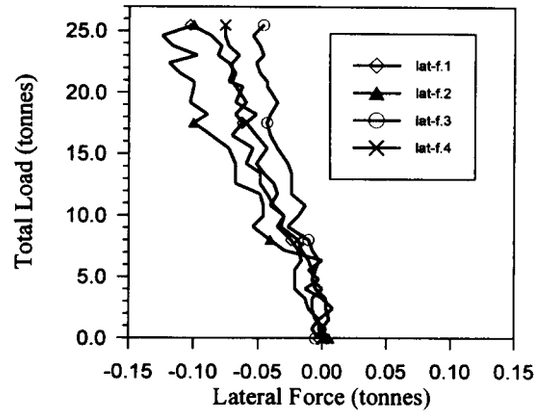

FIG. 17. Lateral Forces Recorded in Scaffold Frame Shoring in Load Path C

loads supported by the scaffold frame shoring are much less than the system critical load.

The total weight of 30 sand bags in these tests corresponds to the weight of a fresh 20-cm-thick concrete slab, which is typically used in actual construction sites. The lateral forces and displacements of the scaffold frame shoring in these tests can be applied to reflect the truth of actual construction sites (Huang and Chen 1996).

Check of Test Variances

Effect of Sand Bag Impact

The placed sand bags may induce an impact effect during placing in tests. This impact effect of sand bags needs to be verified to make sure that the recorded data is correct. The test results show that the continuous five set data recorded have few variances, so the impact effect of placing sand bags is not specified (Yen et al. 1995).

Variance of Total Load

The total load was measured by the following two methods: (1) the total load (A) is the sum of all axial tube forces (40 tubes) measured from strain gauges; and (2) the total load (B) is the sum of all sand bags. The weight of each sand bag was measured before tests. The differences in these two methods A and B, are less than 13% (Yen et al. 1995).

CONCLUSIONS

This research mainly investigates the behavior of a full-scale scaffold frame shoring subjected to pattern loads paths. The scaffold frame shoring is erected including the specific installation and loads such as a three-story scaffold frame shoring, discontinuous formwork and stringers, a nonsway boundary condition, adjustable shoring heads on the top of scaffolds, sand bag loading, and so on. Based on the results of those conditions, several conclusions can be drawn from this research.

The effect of influence surfaces in a scaffold frame shoring is not significant during load paths. This is due to the discontinuities existed both in formwork and in stringers placed on the scaffolds. Furthermore, since joints in the scaffold frame shoring are not connected rigidly, this influences the force transmission somewhat.

As soon as the sand bag is placed at a specified location on the formwork, the axial tube force beneath the placed sand bag jumps suddenly. After the jump, it will not change much, when sand bags are placed at other locations.

The maximum axial tube forces with different load paths do

not differ much from that of the uniform load used in a typical design calculation.

Regions of large axial forces are different for various load paths. These regions should be strengthened or considered as a key area of a warning system.

The lateral forces provided to prevent the sway of the top of a scaffold frame shoring are small in different load paths while sand bags are being slowly placed on formwork. This implies that the actual lateral forces transferred to reinforced-concrete walls and columns are not significant in actual construction sites if fresh concrete is slowly placed on formwork.

The lateral displacements of scaffolds are not significant during different load paths in tests. This implies that the horizontal sidesway of the tested scaffold frame shoring is small when the thickness of concrete slab is about 20 cm.

ACKNOWLEDGMENTS

The writers would like to acknowledge the Council of Labor Affairs of Taiwan and Yu-Shu Construction Company for their support of this research. The writers also appreciate H. J. Chen, W. L. Tsi and C. H. Huang for their help in this full-scale test.

APPENDIX. REFERENCES

Hadipriono, F. C., and Wang, H. K. (1986). "Analysis of causes of formwork failures in concrete structures." *J. Constr. Engrg. and Mgmt.*, ASCE, 112(1), 112–121.

Huang, Y. L., Yen, T. and Chen W. F. (1996). "A monitoring system for high-clearance scaffold systems during construction." *Proc. of Structures Congress XVI*, ASCE, April 15–18, Chicago, Ill., 719–726.

Jirsa, J. O., Sozen, M. A., and Siess, C. P. (1969). "Pattern loadings on reinforced concrete floor slabs." *J. Struct. Div.*, ASCE, 96(6), 1117–1137.

Jofriet, J. C., and McNeice, G. M. (1971). "Pattern loading on reinforced concrete flat plates." *Proc., Am. Concrete Inst.*, Am. Concrete Inst., Detroit, Mich., 68(Dec.), 968–972.

Peng, J. L. (1994). "Analysis models and design guidelines for high-clearance scaffold systems," PhD thesis, School of Civ. Engrg., Purdue Univ., West Lafayette, Ind., 330.

Peng, J. L., Pan, A. D., Rosowsky, D. V., Chen, W. F., Yen, T., and Chan, S. L. (1996a). "High clearance scaffold systems during construction, part I: structural modeling and modes of failure." *Engrg. Struct.*, 18(3), 247–257.

Peng, J. L., Rosowsky, D. V., Pan, A. D., Chen, W. F., Chan, S. L., and Yen, T. (1996b). "High clearance scaffold systems during construction, part II: structural analysis and development of design guidelines." *Engrg. Struct.*, 18(3), 258–267.

Peng, J. L., Rosowsky, D. V., Pan, A. D., Chen, W. F., Chan, S. L., and Yen, T. (1996c). "Analysis of concrete placement load effects using influence surfaces." *ACI Struct. J.*, 93(2), 180–186.

Yen, T., Chu, M. S., Go, C. G., Lin, C. H., Lin, C. C., Huang, Y. L., and Peng, J. L. (1991). "Safety evaluation and checklists of falsework and scaffolding." *Rep. 03-41-05*, Council of Labor Affairs, Taipei, Taiwan (in Chinese).

Yen, T., Lin, C. H., Go, C. G., Chu, M. S., Huang, Y. L., Chen, H. J., Chen, W. F., Rosowsky, D. V., Pan, A. D., and Huang, C. H. (1993). "Safety study of steel scaffold temporary structures during construction." *Rep.*, Council of Labor Affairs, Taipei, Taiwan (in Chinese).

Yen, T., Chen, W. F., Lin, Y., Huang, Y. L., Chen, H. J., and Peng, J. L. (1995). "Study of the interaction between wooden shores and steel scaffolds and development of collapse warning system." *IOSH84-S121*, Council of Labor Affairs, Taipei, Taiwan (in Chinese).